THE JOURNAL OF PHYSICAL CHEMISTRY B

Article

pubs.acs.org/JPCB

Ion Transport through Ultrathin Electrolyte under Applied Voltages

Zhen Cao, Yuxing Peng, and Gregory A. Voth*

Department of Chemistry, James Franck Institute, Computation Institute, The University of Chicago, 5735 South Ellis Avenue, Chicago, Illinois 60637, United States

ABSTRACT: The influence of the Coulomb transport (CT) effect on ion transport in electrolytes is evaluated through two prototypical systems: the $[IrCl_6]^{2-/3-}$ redox couple in aqueous solution and Mg^{2+} (with $TFSI^-$ counterions) in acetonitrile solution. In the first system, transport of the $[IrCl_6]^{2-/3-}$ anions is inhibited, and ions are trapped near the positive electrode due to the unscreened electric field. With larger applied voltage, the inhibition is stronger. This effect can be weakened, however, by adding supporting charges, which screen the electric field of the electrodes. In the second system, the unscreened electric field provides a means of separating $[Mg_x(TFSI)_y]^{(2x-y)+}$ clusters in the electrolyte. This effect enhances charge transport by providing a larger number of faster-moving (smaller) ions. Considered together, these systems provide examples of how the CT effect may increase or decrease charge transport and how one might attempt to modulate this effect in order to enhance electrochemical cell conduction.

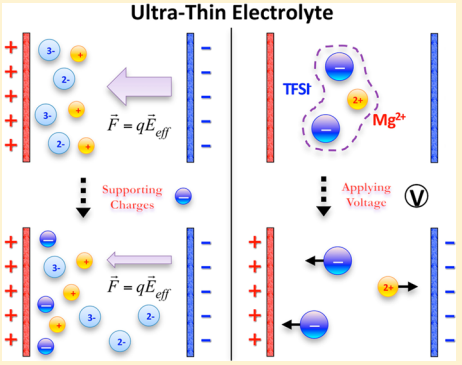

1. INTRODUCTION

Ion transport is essential in electrochemical cells. Studies indicate that the efficiency of this process is attributable primarily to the intrinsic properties of electrolytes, which mediate the interactions between charge carriers and other cell components. On the basis of this understanding, a great deal of research has focused on screening systems in order to improve performance. Successful examples include materials consisting of small organic molecules[1,2] or polymers,[3−7] which form loose solvation shells that allow ions to migrate easily. Meanwhile, simulations[8−10] have quantitatively explored the relationship between electrolyte structure and activity, with the goal of guiding rational design of electrolytes. Despite some progress, ion diffusion remains one of the rate-limiting steps in cell conduction[11,12] (being slower than, e.g., electron transfer between the electrolyte and electrode surface). Hence, the insights gleaned from studies of ion transport hold promise for further improving the performance of electrochemical cells.

Recently, it has been proposed that the Coulomb transport (CT) effect can strongly influence ion transport in electrochemical cells.[13,14] The CT effect arises when two electrodes are sufficiently close to each other that the electric field originating from the electrodes cannot be fully screened by electrolyte molecules; in this case, the unscreened electric field can drive ion transport, greatly increasing cell efficiency. Exploiting this effect hinges on the design of cell structures, rather than of electrolytes. Therefore, in principle, redesigning electrochemical cells to take advantage of CT promises to increase performance (e.g., by raising the power density) while maintaining all of the benefits of previous improvements to electrolytes. Moreover, fully understanding the mechanism behind CT should prove instructive for further applications in real electrochemical cell design. A previous study[14] also examined this effect using multiconfigurational reactive molecular dynamics simulations of proton transport in thin (∼6 nm) layers of aqueous electrolyte and found that the H^+ migration rate increases almost linearly with the applied voltage. The result is consistent with the concept that high power output can be achieved using partially screened electric fields.

In this work, the influence of the CT effect on ion transport is further explored through the examination of two other prototypical systems. The first system consists of the $[IrCl_6]^{2-/3-}$ redox couple in ultrathin aqueous electrolyte between two platinum electrodes. The CT effect is illustrated by investigating the transport behavior of this redox couple under a range of applied voltages. In addition, it is shown that the CT effect can be adjusted by varying the concentration of supporting charges, which screen the electric field of the electrodes. The second system consists of $Mg[TFSI]_2$ (TFSI is bis(trifluoromethanesulfonyl)-imide) in an acetonitrile solution ultrathin electrolyte under applied voltages. Mg^{2+} can be used as a charge carrier for a possible cheaper, safer alternative to the lithium ion battery.[15] In this work, the effect of applied voltage on the Mg^{2+} solvation structure is probed. With no applied field, Mg^{2+} and $TFSI^-$ tend to cluster;[16,17] it is proposed that unscreened electric fields may separate these clusters, improving the efficiency of ion transport.

The remainder of this work will be structured as follows: in section 2, the methodology, including the polarizable electrode model and the system setup, is described. Results are next

Special Issue: John R. Miller and Marshall D. Newton Festschrift

Received: November 10, 2014
Revised: January 3, 2015

DOI: 10.1021/jp511260v
J. Phys. Chem. B XXXX, XXX, XXX−XXX

presented in section 3, and it is discussed in detail how best to exploit the CT effect. In addition, a set of straightforward experiments for testing the simulation results is described. In section 4, a short conclusion summarizes how the CT effect can influence ion transport in ultrathin electrolytes and discusses the consequences for electrochemical cell design.

2. METHODOLOGY AND SYSTEM SETUP

2.1. Polarizable Electrode Model. To correctly describe the behavior of atoms in ultrathin electrolyte, it is necessary to employ a polarizable electrode model because the interfacial particles that are strongly affected by polarization constitute a large percentage of the system. Therefore, in this study, a polarizable electrode model[13] previously described is employed. The development and validation of this model are discussed elsewhere;[13] here, only a brief summary of the model is presented. The model originates from the image charge concept of electrostatics. Consider a particle with partial charge q_i located between two ideal conducting planes, which are separated by distance D. The particle will induce two primary image charges $-q_i$ on the other side of the planes, which will in turn induce higher-order image charges recursively. All of the higher-order image charges can be represented in terms of $Q_{LE} = q_i z_i/D$ and $Q_{RE} = q_i(D - z_i)/D$, where Q_{LE} and Q_{RE} represent the higher-order image charges distributed on the left and right electrode, respectively, and z_i is the distance between the charge q_i and left electrode surface. An external voltage ΔV can be applied by adding equal but opposite effective charges to both electrode surfaces through the ideal capacitor equation, $Q_{eff} = \Delta V A \varepsilon_0/D$, where A is the area of the electrode surface and ε_0 is the vacuum permittivity.

2.2. System Setup. Two representative systems are examined in this study, the $[IrCl_6]^{2-/3-}$ redox couple in aqueous phase electrolyte and Mg^{2+} in a nonaqueous phase electrolyte ($TFSI^-$ counterion and acetonitrile as the solvent) under a range of applied voltages. For the first system, 6 $[IrCl_6]^{2-/3-}$ anions[18] were placed in a cubic box with 2591 SPC/Fw water[19] molecules, and Na^+ counterions[20] were added to neutralize the solution. To adjust the strength of the CT effect, $NaNO_3$[21] was added to the electrolyte in concentrations ranging from 0.1 to 1 M. The simulations were performed using an in-house code coupled to the LAMMPS package.[22] The aqueous solutions were equilibrated in the constant *NPT* ensemble[23] at 300 K and 1 atm using a Nose−Hoover thermostat and barostat with a 100 fs temperature damping parameter and 1 ps pressure damping parameter at 1 atm and 300 K for 2 ns. The last 1 ns of each trajectory was used to calculate the average volume. The solutions were then placed between two platinum electrodes toward the platinum (111) surfaces, whose Lennard-Jones (L-J) parameters were obtained from our previous simulations.[13] A three-body interaction[24] between the water molecules and the platinum atoms was also employed. Dispersion interactions between electrodes and ions were described by the L-J potentials using the Lorentz−Berthelot combination rules. The long-range electrostatic interactions were calculated by using the particle−particle particle-mesh (PPPM) method[25] with slab correction[26] added along the z direction. To equilibrate the system under external voltages, a 5 V potential was first applied across the electrodes, and each system was simulated in the constant *NVT* ensemble[27] at 300 K for 5 ns using a Nose−Hoover thermostat with a 100 fs temperature damping parameter to accelerate the equilibration considering the relative slow diffusion rate of the large anions in solution. Finally, the systems were equilibrated in the constant *NVT* ensemble[27] for 10 ns using a 1 fs time step at potentials of 0.25, 0.5, and 1 V, respectively, until the distribution of the anions was fully converged. This procedure was also tested to be independent of the initial applied voltage in the first step, which only served to speed up the equilibration phase. Then, 20 ns trajectories were used for the analysis of static properties. For the analysis of dynamical properties, five different configurations were selected from the equilibrated trajectory at each applied voltage, 2 ns simulations in the constant *NVE* ensemble were performed for each configuration with a 1 fs time step, and the coordinates were recorded every 100 fs.

For the second system, 0.3 M $Mg[TFSI]_2$[28] in acetonitrile solution[29] was equilibrated in the constant *NPT* ensemble[23] using the Nose−Hoover thermostat and barostat at 300 K and 1 atm with a 100 fs temperature damping parameter and 1000 fs pressure damping parameter for 2 ns, and the last 1 ns trajectory was used to obtain the average volume; the solution was then inserted between two platinum (111) surfaces, as for the previous system. The dispersion interactions between electrolyte and electrodes were described using the L-J potential with the Lorentz−Berthelot combination rules. Then, the systems were equilibrated in the constant *NVT* ensemble[27] using Nose−Hoover thermostat with a 100 fs damping parameter at 300 K for 50 ns. A total of 30 different configurations were chosen from the last 20 ns of this trajectory; these were simulated in the constant *NVE* ensemble under applied potentials of 1, 2, and 4 V for the analysis of the system properties, and the coordinates were recorded every 100 fs.

3. RESULTS AND DISCUSSION

3.1. $[IrCl_6]^{2-/3-}$ in Aqueous Electrolyte. In order for an $[IrCl_6]^{2-/3-}$ cell to generate a current, it is necessary for $[IrCl_6]^{3-}$ anions to diffuse against the electrostatic potential to the negative electrode to be oxidized to $[IrCl_6]^{2-}$. However, the ultrathin electrolyte cannot fully shield the applied electric field, which opposes the migration of $[IrCl_6]^{3-}$ anions to the negative electrode and traps them near the positive electrode. As a result, the CT effect will decrease the redox reaction rate by lowering the number of anions near the negative electrode. In an experimental current−voltage curve, one would expect a smaller peak current at higher voltage. In the following, this expectation is tested using three metrics: the anion diffusion constant, the anion density profile, and the properties that originated from the Poisson equations.

If higher voltage decreases charge transport, one would expect higher voltage to lead to decreased anion diffusion coefficients. In Figure 1, therefore, we plot the effective diffusion constants of the $[IrCl_6]^{2-/3-}$ anions' centers of mass (COMs) in the z direction (normal to the electrode planes), computed from the one-dimensional mean-square displacement using the formula $D_{eff} = \langle |r^z_{COM}(t) - r^z_{COM}(0)|^2 \rangle / 2t$. In general, the effective diffusion coefficients are smaller than those for bulk solution, supporting the idea that the CT effect can change the dynamical properties of ion transport in the ultrathin electrolyte layer. It is also notable that with increased applied voltage, the effective diffusion coefficients are progressively smaller, indicating that the CT effect inhibits the ion transport in the electrolyte.

To improve the ion transport efficiency, one can however add supporting charges into electrolytes to shield the electric

DOI: 10.1021/jp511260v
J. Phys. Chem. B XXXX, XXX, XXX−XXX

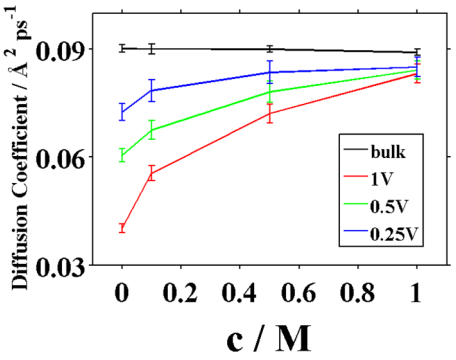

Figure 1. Effective diffusion coefficients of the redox couple in aqueous solution with 0, 0.1, 0.5, and 1 M supporting charges under 0.25, 0.5, and 1 V applied voltages. The bulk value is also shown as a benchmark.

field. This effect is displayed in Figure 1 by diffusion constants for solutions with 0.1−1 M added $NaNO_3$. Because the electrostatic fields generated by these ions are stronger than those generated by water, one may expect that added $NaNO_3$ will weaken the CT effect. Indeed, it is very clear that adding salt increases the effective diffusion coefficient, which approaches the bulk value for 1 M added $NaNO_3$. Experimentally, one could validate these conclusions using cyclic voltammetry experiments. Because the migration of the redox couple is accelerated by adding the supporting charges, the electrochemical reactions rate would be increased, leading to a higher peak value in the current−voltage curve.

From the hypothesis that the decreased migration rate of $[IrCl_6]^{2-/3-}$ is the result of the CT effect, one also expects that anions will be trapped near the positive electrode; this can be detected from the density profile of anions along the z direction under different conditions. The results are shown in Figure 2. The high peak near the positive electrode demonstrates the expected CT effect. As supporting charges are added, the CT effect is weakened, and the height of this peak decreases. Although this property is difficult to characterize directly using experiments, greater density buildup near the positive electrode should correlate with decreased electrochemical reaction rates, which can be measured using cyclic voltammetry experiments.

Because the most direct implication of the CT effect regards the presence of an unshielded electric field throughout the electrolyte, one way to reveal this phenomenon is to calculate the Poisson potential in the electrolyte under different conditions. This property can be evaluated using the equation $\nabla^2\Phi(z) = -\rho(z)/\varepsilon_0$, where $\rho(z)$ is the charge density along the z direction and ε_0 is the vacuum permittivity. The results are shown in Figure 3. The pronounced fluctuations of the Poisson potential near the electrodes correspond to the double layer due to the strong interaction between the electrolyte and electrodes, which is well represented by the polarizable electrode model using the image charge method.[13,30] In the middle region, the electric potential is flatter, and the slope of the potential corresponds to the unscreened electric field. In general, the slope of Poisson potential in the middle region is larger with increasing applied voltage. By adding the supporting charges, the electric field can be effectively shielded, and the slope becomes smaller. The Poisson potential throughout the ultrathin electrolyte can directly provide the relationship between the CT effect and the applied voltage and is related to the distribution of supporting charges, which generate the

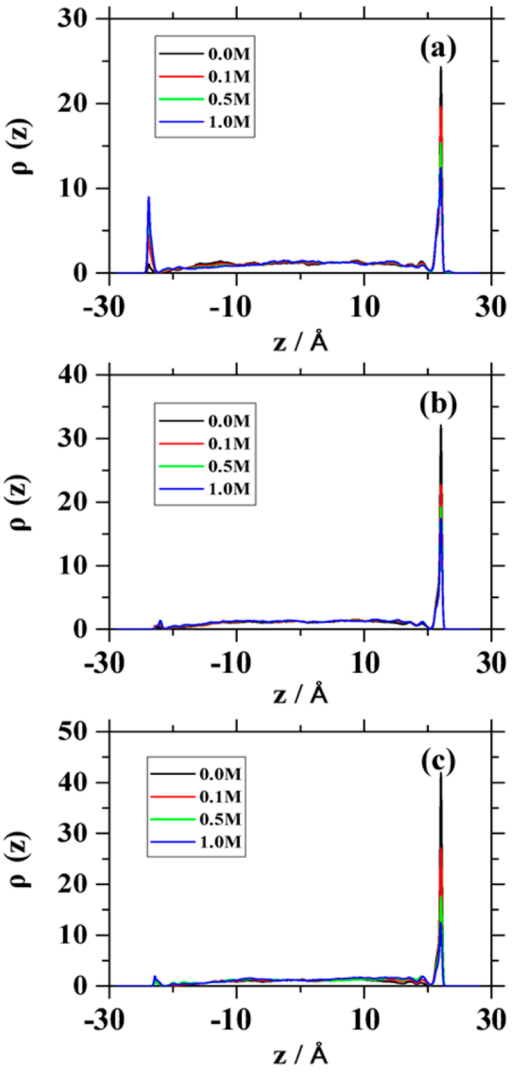

Figure 2. Density profile of the $[IrCl6]^{2-/3-}$ in the aqueous electrolyte under (a) 0.25, (b) 0.5, and (c) 1 V applied voltages.

shielding effects. As an alternative, the Debye length,[31] a parameter for evaluating the screening effect, is calculated for different systems using $\lambda = (\varepsilon_0\varepsilon_r k_B T/\sum_i c_i q_i^2)^{1/2}$, where k_B is the Boltzmann constant, T is the temperature, and c_i and q_i are the concentration and the ionic charge of the ith ion. In practice, the electric field will decay to 1% within five Debye lengths; in our calculation, the percentage of the sample volume within five Debye lengths of the electrodes is 76% with no supporting charge or 45% with 1 M supporting charge. Considered together, these results imply that for redox couples of the same charge, one can improve electrochemical cell efficiency by minimizing the CT effect, for example, by adding supporting electrolytes.

3.2. Mg^{2+} in Acetonitrile Electrolyte. The second prototypical system chosen here is $Mg[TFSI]_2$ in acetonitrile solution. A potential problem with this system is that Mg^{2+} can easily form clusters with $TFSI^-$ anions[16,17] because the low polarizability of the acetonitrile solution makes it a worse solvent than, for example, water. Due to their lowered charge density as compared to Mg^{2+} cations, Mg^{2+} clusters do not support efficient charge transport. In this case, however, we expect that the CT effect may enhance charge transport because the unscreened electric field will drive Mg^{2+} cations

DOI: 10.1021/jp511260v
J. Phys. Chem. B XXXX, XXX, XXX−XXX

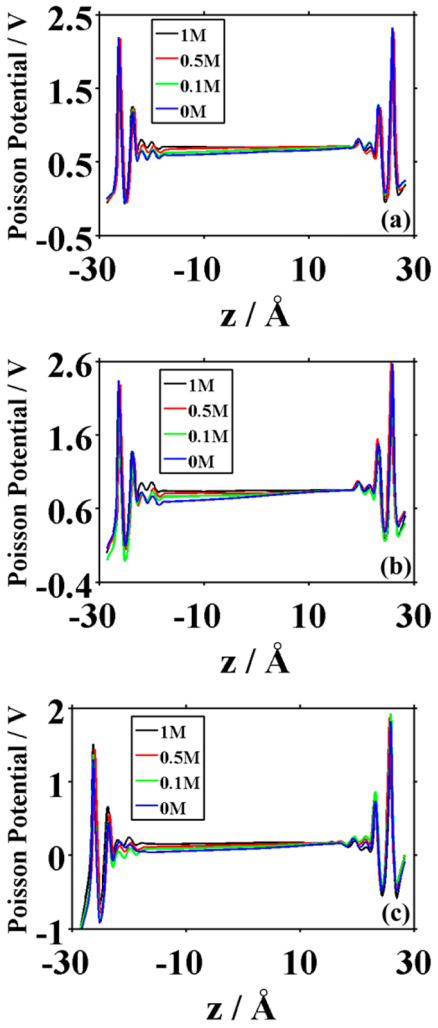

Figure 3. Poisson potential drop through the electrolyte under (a) 0.25, (b) 0.5, and (c) 1 V applied voltages.

and $TFSI^-$ anions in opposite directions, helping to separate clusters in the electrolyte. Below, we directly characterize the CT effect on ion clustering using Voronoi analysis and subsequently describe its effect on charge transport by calculating diffusion limits and Poisson potentials.

The cluster formation of the Mg^{2+} cations and $TFSI^-$ anions can be directly investigated using the Voronoi analysis.[32,33] In Voronoi analysis, the simulation box is divided into three-dimensional polyhedral cells, which correspond roughly to the space occupied by each particle. Two molecules are considered to be neighbors when their Voronoi cells share three vertices. $[Mg_x(TFSI)_y]^{(2x-y)+}$ clusters, then, consist of a group of neighboring Voronoi cells containing Mg^{2+} or $TFSI^-$, surrounded by cells containing acetonitrile. The percentage of the Mg^{2+} forming the different sizes of clusters as a function of the applied potential is shown in Figure 4. As anticipated, higher voltages correspond to more separated ions and a higher percentage of smaller clusters and bare Mg^{2+} cations.

To characterize the influence of the CT effect on ion transport, the diffusion limit of the current (I_{lim}) is now calculated. This quantity, which takes into account the effects of both ion diffusivity and clustering on charge transport, is calculated using the formula $I_{lim} = \sum_i n_i A D_i^{eff} F C_i / d$, where A is the surface area of the electrode, d is the distance between two

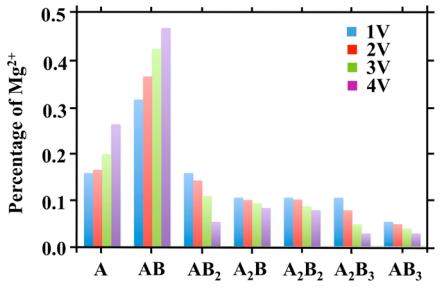

Figure 4. Distribution of Mg^{2+} forming different sizes of the $[Mg_x(TFSI)_y]^{(2x-y)+}$ clusters in the acetonitrile electrolyte at different applied voltages. A represents Mg^{2+}, and B represents $TFSI^-$ in the figure.

electrodes, F is the Faraday constant, D_i^{eff} is the effective diffusion coefficient for the ith cluster along the z direction (normal to the electrode planes), C_i is the concentration of the ith cluster, and n_i is the net charge of the ith cluster. In general, the faster cluster with larger net charge contributes more to the current. The ratio of effective current at different applied voltages to the diffusion limit in a bulk system is shown in Figure 5. It is interesting that with higher applied voltage, the

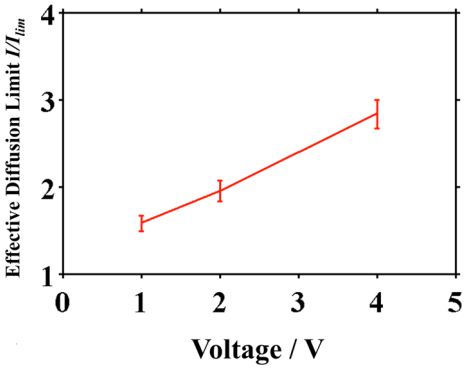

Figure 5. Ratio of the effective current of the $[Mg_x(TFSI)_y]^{(2x-y)+}$ clusters to the current due to bulk diffusion at 1, 2, and 4 V applied voltages.

current is much larger. This can be explained in two ways. First, consistent with our previous study of proton transport in aqueous solution,[14] the unscreened electric field may drive faster cation diffusion. In addition, the unscreened electric field may help to separate the ion clusters, such that the electrolyte consists of a larger number of faster-moving charges.

Finally, the Poisson potential throughout the electrolyte is calculated; the results for different conditions are shown in Figure 6. The pronounced fluctuations near the electrodes again correspond to the electrical double layer, which is well represented by the polarizable electrode model,[13,30] and the slope of the flatter line in the middle of the cell indicates the strength of the unscreened electric field. In general, larger slopes are observed as compared to those shown in Figure 3; this is mainly because the screening capacity of acetonitrile is smaller than that of water, which is consistent with the smaller dielectric constant for acetonitrile (26 for this acetonitrile model[29]) as compared to water (80 for SPC/Fw water[19]). With higher applied voltages, the slope of the curves in the middle region is larger, indicating an enhanced CT effect. Because the CT effect enhances charge transport in this case, these results exemplify how the CT effect may be used to improve the

DOI: 10.1021/jp511260v
J. Phys. Chem. B XXXX, XXX, XXX−XXX

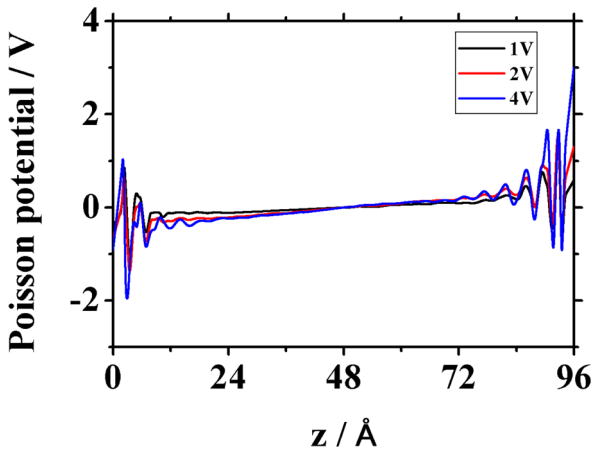

Figure 6. Poisson potential drop through the electrolyte under 1, 2, and 4 V applied voltages.

electrochemical cell efficiency without requiring the synthesis of new electrolyte components.

4. CONCLUSIONS

In this work, the influence of the CT effect on ion transport in the ultrathin electrolytes has been investigated using two representative systems, $[IrCl_6]^{2-/3-}$ in water and $Mg[TFSI]_2$ in acetonitrile. In the first system, both members of the redox couple carry a charge of the same sign, and these ions can become trapped near one electrode due to the CT effect. This effect can be mitigated by adding supporting charges into the electrolyte. In the second system, the primary problem is the clustering of ions with unlike signs. Because the CT effect leads to forces in opposite directions for cations and anions, it may be exploited to help to separate these clusters and improve the ion transport efficiency. Together, then, these studies present a framework for evaluating whether the CT effect is likely to be detrimental or beneficial for enhancing conductance in a given electrochemical cell. Because the modulation of the CT effect hinges on the design of cell structures rather than of new materials, this study offers a useful perspective for enhancing cell performance, and further validation and applications of the conclusions presented here may be expected.

AUTHOR INFORMATION

Corresponding Author

*E-mail: gavoth@uchicago.edu.

Notes

The authors declare no competing financial interest.

ACKNOWLEDGMENTS

This research was supported by the Office of Naval Research (ONR Grant N0014-12-1-1021). The computations in this work were partially completed with resources provided by the University of Chicago Research Computing Center (RCC). We thank Prof. Henry White for valuable discussions.

REFERENCES

(1) Xu, K. Nonaqueous Liquid Electrolytes for Lithium-Based Rechargeable Batteries. *Chem. Rev.* **2004**, *104*, 4303−4417.
(2) Scheers, J.; Fantini, S.; Johansson, P. A Review of Electrolytes for Lithium−Sulphur Batteries. *J. Power Source* **2014**, *255*, 204−218.
(3) Pan, J.; Chen, C.; Zhuang, L.; Lu, J. T. Designing Advanced Alkaline Polymer Electrolytes for Fuel Cell Applications. *Acc. Chem. Res.* **2012**, *45*, 473−481.
(4) Borup, R.; et al. Scientific Aspects of Polymer Electrolyte Fuel Cell Durability and Degradation. *Chem. Rev.* **2007**, *107*, 3904−3951.
(5) Zhang, H.; Shen, P. K. Recent Development of Polymer Electrolyte Membranes for Fuel Cells. *Chem. Rev.* **2012**, *112*, 2780−2832.
(6) Wang, Y. J.; Qiao, J. L.; Baker, R.; Zhang, J. J. Alkaline Polymer Electrolyte Membranes for Fuel Cell Applications. *Chem. Soc. Rev.* **2013**, *42*, 5768−5787.
(7) Mauritz, K.; Moore, R. B. State of Understanding of Nafion. *Chem. Rev.* **2004**, *104*, 4535−4586.
(8) Weber, A. Z.; Newman, J. Modeling Transport in Polymer−Electrolyte Fuel Cells. *Chem. Rev.* **2004**, *104*, 4679−4726.
(9) Wang, C. Fundamental Models for Fuel Cell Engineering. *Chem. Rev.* **2004**, *104*, 4727−4766.
(10) Jorn, R.; Savage, J.; Voth, G. A. Proton Conduction in Exchange Membranes across Multiple Length Scales. *Acc. Chem. Res.* **2012**, *45*, 2002−2010.
(11) Hu, Y.; Adelhelm, P.; Smarsly, B. M.; Hore, S.; Antonietti, M.; Maier, J. Synthesis of Hierarchically Porous Carbon Monoliths with Highly Ordered Microstructure and Their Application in Rechargeable Lithium Batteries with High-Rate Capability. *Adv. Funct. Mater.* **2007**, *17*, 1873−1878.
(12) Peng, B.; Cheng, F.; Tao, Z.; Chen, J. Lithium Transport at Silicon Thin Film: Barrier for High-Rate Capability Anode. *J. Chem. Phys.* **2010**, *133*, 034701.
(13) Petersen, M. K.; Kumar, R.; White, H. S.; Voth, G. A. A Computationally Efficient Treatment of Polarizable Electrochemical Cells Held at a Constant Potential. *J. Phys. Chem. C* **2012**, *116*, 4903−4912.
(14) Cao, Z.; Kumar, R.; Peng, Y.; Voth, G. A. Proton Transport under External Applied Voltage. *J. Phys. Chem. B* **2014**, 8090−8098.
(15) Saha, P.; Datta, M. K.; Velikokhatnyib, O. I.; Manivannana, A.; Almana, D.; Kumta, P. N. Rechargeable Magnesium Battery: Current Status and Key Challenges for the Future. *Prog. Mater. Sci.* **2014**, *66*, 1−86.
(16) Giffin, G. A.; Moretti, A.; Jeong, S.; Passerini, S. Complex Nature of Ionic Coordination in Magnesium Ionic Liquid-Based Electrolytes: Solvates with Mobile Mg^{2+} Cations. *J. Phys. Chem. C* **2014**, *118*, 9966−9973.
(17) Kumar, Y.; Hashmi, S. A.; Pandey, G. P. Ionic Liquid Mediated Magnesium Ion Conduction in Poly(ethylene oxide) Based Polymer Electrolyte. *Electrochim. Acta* **2011**, *56*, 3864−3873.
(18) Tubert-Brohman, I.; Schmid, M.; Meuwly, M. Molecular Mechanics Force Field for Octahedral Organometallic Compounds with Inclusion of the Trans Influence. *J. Chem. Theory Comput.* **2009**, *5*, 530−539.
(19) Wu, Y.; Tepper, H. L.; Voth, G. A. Flexible Simple Point-Charge Water Model with Improved Liquid-State Properties. *J. Chem. Phys.* **2006**, *124*, 024503.
(20) Joung, I. S.; Cheatham, T. E. I. Determination of Alkali and Halide Monovalent Ion Parameters for Use in Explicitly Solvated Biomolecular Simulations. *J. Phys. Chem. B* **2008**, *112*, 9020−9041.
(21) Guilbaud, P.; Wipff, G. Force Field Representation of the UO_2^{2+} Cation from Free Energy MD Simulations in Water. Tests on Its 18-Crown-6 and NO_3^- Adducts, and on Its Calix[6]Arene^{6-} and CMPO Complexes. *J. Mol. Struct.: THEOCHEM* **1996**, *366*, 55−63.
(22) Plimpton, S. Fast Parallel Algorithms for Short-Range Molecular Dynamics. *J. Comput. Phys.* **1995**, *117*, 1−19.
(23) Berendsen, H. J. C.; Postma, J. P. M.; van Gunsteren, W. F.; DiNola, A.; Haak, J. R. Molecular Dynamics with Coupling to an External Bath. *J. Chem. Phys.* **1984**, *81*, 3684.
(24) Siepmann, J. I.; Sprik, M. Influence of Surface Topology and Electrostatic Potential on Water/Electrode Systems. *J. Chem. Phys.* **1995**, *102*, 511−524.
(25) Hockney, R. W.; Eastwood, J. W. *Computer Simulation Using Particles*; Adam Hilger: New York, 1989.

DOI: 10.1021/jp511260v
J. Phys. Chem. B XXXX, XXX, XXX−XXX

(26) Yeh, I.; Berkowitz, M. L. Ewald Summation for Systems with Slab Geometry. *J. Chem. Phys.* **1999**, *111*, 3155−3162.
(27) Nose, S. A Unified Formulation of the Constant Temperature Molecular Dynamics Methods. *J. Chem. Phys.* **1984**, *81*, 511−519.
(28) Li, S.; et al. Molecular Dynamics Simulation of LiTFSI−Acetamide Electrolytes: Structural Properties. *J. Phys. Chem. B* **2008**, *112*, 6398−6410.
(29) Nikitin, A. M.; Lyubartsev, A. P. New Six-Site Acetonitrile Model for Simulations of Liquid Acetonitrile and Its Aqueous Mixtures. *J. Comput. Chem.* **2007**, *28*, 2020−2026.
(30) Calhoun, A.; Voth, G. A. Electron Transfer across the Electrode/Electrolyte Interface: Influence of Redox Ion Mobility and Counterions. *J. Phys. Chem.* **1996**, *100*, 10746−10753.
(31) Robinson, R. A.; Stokes, R. H. *Electrolyte Solutions*, 2nd revised ed.; Butterworth & Co. Ltd.: London, 2002.
(32) Barber, C. B.; Dobkin, D. P.; Huhdanpaa, H. T. The Quickhull Algorithm for Convex Hulls. *ACM Trans. Math. Software* **1996**, *22*, 469−483.
(33) Raschke, T. M.; Levitt, M. Nonpolar Solutes Enhance Water Structure within Hydration Shells while Reducing Interactions between Them. *Proc. Natl. Acad. Sci. U.S.A.* **2005**, *102*, 6777−6782.

DOI: 10.1021/jp511260v
J. Phys. Chem. B XXXX, XXX, XXX−XXX